

Preparation and Characterization of Cross-linked Chitosan Microcapsules for Controlled Delivery of Oxytetracycline

O. LARBI-BOUAMRANE, Y. BAL*, D. ALIOUCHE¹, G. COTE² AND A. CHAGNES²

Laboratory of Molecular and Macromolecular Physical Chemistry, University of Blida I, 09000 Blida, Algeria, ¹Laboratory of Fibrous Polymers Treatment and Forming, University of Boumerdes, 35000 Boumerdes, Algeria, ²Institut de Recherche de Chimie Paris, CNRS-Chimie Paris Tech, 11 rue Pierre et Marie Curie, 75005 Paris, France

Larbi-Bouamrane, *et al.*: Preparation of Chitosan Microcapsules for Delivery of Oxytetracycline

Formulations of encapsulated oxytetracycline in chitosan spherical beads have been developed in this work through the ionotropic gelation method in sodium tripolyphosphate or hexametaphosphate and characterized as drug delivery system to the gastrointestinal tract by Fourier transform infrared spectroscopy, thermal analysis and *in vitro* drug release in simulated gastric fluids. The Fourier transform infrared spectroscopy and differential scanning calorimetry measurements showed that tripolyphosphate and hexametaphosphate are cross-linked ionically to chitosan and there was no significant drug interaction between the entrapped drug and the carrying polymer. With respect to chitosan cross-linking features, sodium hexametaphosphate seems to give better swelling, higher diffusion and faster release kinetics, while addition of glutaraldehyde as a second cross-linking agent lowers the drug discharge. Release extent and kinetics were found to be pH dependent and approximated very well by the multistep models equations of Makoid-Banakar, Peppas-Sahlin and Korsmeyer-Peppas.

Key words: Oxytetracycline, chitosan, encapsulation, crosslinking, release kinetics

Tetracyclines are broad spectrum antibiotics that exhibit activity against a wide range of Gram-positive and Gram-negative bacteria. Their favourable antimicrobial properties and the absence of major adverse effects have led to their extensive use in the therapy of human and animal infections^[1-4]. Unfortunately, like the other antibiotic and as a result of the extensive prescription in conventional formulations, the emergence of microbial resistance has limited their effectiveness. So, other strategies are needed to keep tetracycline's and other antibiotics as resources for the next generation and to restore their initial antimicrobial activity. These strategies are based on the development of new classes of drugs with unique antibacterial mechanisms or new formulations enabling the reduction of amounts of antimicrobials used worldwide. In particular, investigation of new formulations has been carried out in order to overcome the disadvantages resulting from the administration of antibiotics in conventional forms^[5-7].

The specific addressing of active molecules to the organ, tissue or cell is considered now as a major challenge and promising route for the treatment of

various human diseases, including bacterial infections, cancer or genetic diseases^[8]. New carrying and targeting approaches for drug delivery have been extensively studied in recent years. Most of them are centered on the development of nano- or micro-scale carrying systems^[9-11] or specific molecules to improve and maximize drug bioavailability and hence therapeutic effects over a period of time. This highly selective approach would ensure an optimum response from the dosage form which significantly lowers the side effects and reduce treatment's expense.

As non-conventional pharmaceutical dosage forms, polymer-based drug delivery systems may be designed as safe and effective carrying systems to reach the targeted properties, for example, by improving the solubility of the active agent in specific environments.

This is an open access article distributed under the terms of the Creative Commons Attribution-NonCommercial-ShareAlike 3.0 License, which allows others to remix, tweak, and build upon the work non-commercially, as long as the author is credited and the new creations are licensed under the identical terms

*Address for correspondence

E-mail: bal_y@yahoo.fr

Natural biopolymers such as chitosan or alginate and their derivatives have attracted considerable interest in a wide range of biomedical and pharmaceutical applications including drug delivery and tissue engineering^[12-15]. Several advantages including healing properties, biocompatibility, availability, biodegradability and non-toxicity^[16-18] made them suitable for pharmaceutical preparations. Solutions of these biopolymers are frequently gelled through the ionotropic gelation (IG) method with appropriate cross-linking agents like glutaraldehyde and glyoxal^[19,20] which may be associated with toxic effects or sodium tripolyphosphate and sodium hexametaphosphate^[21-23] which are indicated to be safe.

The IG method appears now to be a very promising route for the encapsulation of various hydrophilic and lipophilic substances as well as cells, bacteria and many other materials. It may be simple, attractive and advantageous method that can be fully industrialized. From sustained recent development many workers reported rational characterization with impact on the pharmaceutical properties of systems prepared according to this method^[24-26] or new applications such as fibers like materials^[27] or an onion-like multi-membrane hydrogel structure fabricated via a multi-step interrupted gelation that was able to control the release of both hydrophobic and hydrophilic model drugs^[28].

This study focuses on the preparation and characterization of chitosan microcapsules intended to the carrying and delivering of oxytetracycline as active agent to colon as target organ. Fourier transform infrared spectroscopy (FTIR), thermal gravimetric analysis (TGA) and differential scanning calorimetry (DSC) are used to characterize the prepared delivery systems. Effects of some process parameters such as pH and concentration are examined in relation to release kinetics of the antibiotic in simulated body fluids.

MATERIALS AND METHODS

Kitomer chitosan (CS) powder from prawn shells (*Pandalus borealis*), with a degree of deacetylation (DD) of 88.4%, was purchased from Marinard Biotech (Quebec, Canada). Oxytetracycline hydrochloride (OTC) of pharmacopoeias grade was obtained as a gift sample from S Vidal Antibiotical, Algeria. Sodium tripolyphosphate (TPP) and sodium hexametaphosphate (HMP) of analytical grade were procured from Fluka. All other chemicals were of analytical grade and used as received. Distilled water was used throughout the

study and other reagents were all analytical reagents grade.

Microcapsule preparation:

CS microcapsules were prepared according to the following method. One gram of CS was accurately weighed and dissolved in a 1% (w/v) acetic acid solution. Two hundred and fifty milligrams of OTC equivalent to a theoretical loading of 25% (w/w) was then added at room temperature to the CS solution under stirring until homogenisation is obtained. Fifty millilitres of OTC-CS dispersion was then added drop wise at the rate of one drop per second through a needle of 0.5 mm (gauge 25) into 200 ml of 6% w/v TPP or 6% w/v HMP aqueous solution under stirring. The droplets instantaneously gelled into discrete OTC-CS microcapsules upon contact with the cross-linking agent. The OTC containing microcapsules were left overnight in a dark area to cure. They were then separated with paper filter, washed with water and dried at room temperature. Glutaraldehyde (GLU) as a second cross-linking agent was added according to three ways; in the first, it was added by mixing the dispersion of OTC in CS with GLU (0.01%) HMP solution giving the (CS/OTC)/(GLU/HMP) formulation. The OTC/CS dispersion was dropped with GLU and the resulting microcapsules were poured in the HMP solution which gave the second formulation (CS/OTC/GLU)/(HMP). The third system was obtained from the subsequent stiffening of the gelled material in HMP in GLU solution giving the (CS/OTC/HMP)/(GLU) formulation.

Drug content of microcapsules:

For the encapsulation efficiency study and prior to the determination of OTC content, the beads were allowed to break during 24 h in aqueous solution of 0.1 N HCl. Tween 80 (0.5%) was added to enhance the drug solubility. The amount of drug was then assayed after filtration by UV/Vis spectrophotometry at 353 nm using Shimadzu 1280 UV/Vis instrument. The determination was made in triplicate and runs averaged. Loading efficiency (%) was calculated using the Eqn. $L(\%) = (W_a/W_t) \times 100$, where W_a is the actual OTC content and W_t is theoretical OTC content.

Swelling tests:

Dried microspheres were carefully weighed and immersed in 50 ml of simulated gastrointestinal fluid (SGF) with pH values ranging from 1.2 to 7.4 at room temperature. At pre-determined time intervals, swollen microspheres were taken out, and the excess water

was blotted with filter paper from the surface, and then weighed on sensitive balance (Sartorius). Below Eqn. was used to determine the swelling degree S (%), which is $S(\%) = ((M_s - M_d) / M_d) \times 100$, where M_d and M_s represent the mass of dry and swollen microspheres, respectively.

Morphological characterization:

Morphological characterization of the microcapsules was carried out by scanning electron microscopy (SEM) using Jeol JSM-6360L instrument. Prior to analysis, the samples were coated with a thin (2 nm) layer of gold.

FTIR spectroscopy:

FTIR spectra of free and encapsulated OTC in CS containing samples were recorded on KBr pellets using Shimadzu 8400 FTIR spectrophotometer (400-4000 cm^{-1}). The samples were thoroughly powdered and dried before milling with anhydrous KBr.

Thermal analysis:

TGA were performed with HR 2950 thermal analysis system (TA Instruments, USA). TGA curves were obtained in the temperature range from 10 to 500°, using platinum crucibles (pan) with 4.0 ± 0.1 mg of sample, under dynamic N_2 atmosphere flowing at 45 ml/min and heating rate of 10°/min. The instrument was preliminarily calibrated at a room temperature using a certified thermometer and by the Curie point with alumel and nickel at 154.16 and 358.28°, respectively. Before test scanning, the air was discharged from the oven at the starting temperature during 3 min.

DSC curves were recorded using the TA 2920 differential scanning calorimeter (TA Instruments, USA) under an inert argon atmosphere at a flow rate of 50 ml/min. The instrument furnace, equipped with two identical crucibles, reference crucible and measurement crucible was preliminarily calibrated for a wide range of working temperature at heating rate of 5° min^{-1} with 5 standard substances (toluene, mercury, gallium, indium and tin). The cell constant calibration was determined with indium. For the current measurements, a test sample is accurately weighed and introduced into the measurement crucible.

In vitro release kinetics:

Prior to drug release kinetic measurements, 0.01 g of dried beads with OTC content were suspended under stirring rate of 50 rpm in 10 ml of simulated

gastrointestinal fluids at pH 7.4 and pH 1.2 and 37°. The simulated intestinal fluid (SIF) of pH 7.4 was composed by a mixture of KH_2PO_4 , NaOH 0.2 N and pancreatin while the SGF of pH 1.2 contained NaCl, HCl and pepsin. Supernatant aliquots of 1 ml were withdrawn periodically and replaced with an equal volume of fresh buffered solution. The amount of OTC released in different media was then determined spectrophotometrically at 353 nm and plotted against time. The *in vitro* release kinetic measurements were performed in triplicate for each sample and in batch mode using conventional magnetic agitator with speed control and thermostated glass vessel.

The release kinetic curves were fitted to various mathematical formulas using appropriate models in which the most reliable models are summarized in Table 1. The modelling procedure was performed using the DD solver add-on tool^[29] working under Microsoft® Excel which can estimate the parameters of a nonlinear function that provides the closest fit between experimental data and the non-linear function. The best fit solution was identified by evaluating the coefficient of correlation (R^2), where the highest R^2 value indicates the best fit. The various parameters derived from fitting models may be used to characterize the release properties and to make pairwise comparisons.

RESULTS AND DISCUSSION

Scanning electron microscopy results in various CS microcapsules materials which are presented in fig. 1. As it is shown, the obtained microcapsules were spherical in shape and seem to have a micro reservoir structure with rough and porous surface. Careful examination demonstrated that the cross-linking procedure plays significant role in the morphology and microstructure of the microcapsules. The surface of the cross-linked microspheres by TPP becomes smooth and more rigid under the subsequent treatment with GLU, the action of which also reduces the size of the resulting microcapsule. Similar observation can be drawn up in the case of HMP which had, previously, flaky and less compact structure as it is depicted in HMP.

FTIR spectroscopy analyzes the infrared spectra of unmodified CS, cross-linked CS (fig. 2). In spectrum (a), a broad absorption band centered around 3437 cm^{-1} is attributed to either the hydrogen bonded O-H or primary amines N-H bonds or both. The polymer also showed characteristic bands at 1651 cm^{-1} attributed to the C=O stretching vibration in amide group and 1596 cm^{-1} arising from the bending vibration of the N-H bonds

TABLE 1: MODEL EQUATIONS USED FOR FITTING DRUG RELEASE DATA

| Model | Equation | Parameter (s) |
|------------------|---|---|
| Higuchi | $Q_t = k_H \cdot t^{0.5}$ | k_H , Higuchi kinetic constant; Q_t is the amount of drug dissolved in time t |
| Weibull 1 | $Q_t = 100 \times [1 - e^{-(t-T_i)^{\beta/\alpha}}]$ | T_i is the location parameter, represents the lag time before the onset of the dissolution or release process and in most of the cases will be zero; α : is the scale parameter defines the time scale of the process; β : characterizes the curves as either exponential ($\beta=1$), S-shaped ($\beta>1$) or parabolic ($\beta<1$) |
| Peppas-Sahlin 1 | $Q_t = k_1 \cdot t^m + k_2 \cdot t^{2m}$ | k_1 : constant that corresponds to the release rate of diffusion; k_2 : constant that corresponds to the release rate of polymer relaxation; m : constant. |
| Peppas-Sahlin 2 | $Q_t = k_1 \cdot t^{0.5} + k_2 \cdot t$ | k_1, k_2 : for diffusion and erosion controlled release; |
| Korsmeyer-Peppas | $Q_t = k_{KP} \cdot t^n$ | k_{KP} : Korsmeyer-Peppas kinetic constant, n : is the release exponent, indicative of the drug release mechanism |
| Baker-Lonsdale | $3/2[1 - (1 - Q_t/100)^{2/3}] - Q_t/100 = k_{BL} \cdot t$ | k_{BL} : Baker-Lonsdale release kinetic constant |
| Makoid-Banakar | $Q_t = k_{MB} \cdot t^n e^{-k \cdot t}$ | k_{MB} : Makoid-Banakar kinetic constant; k, n : constants |

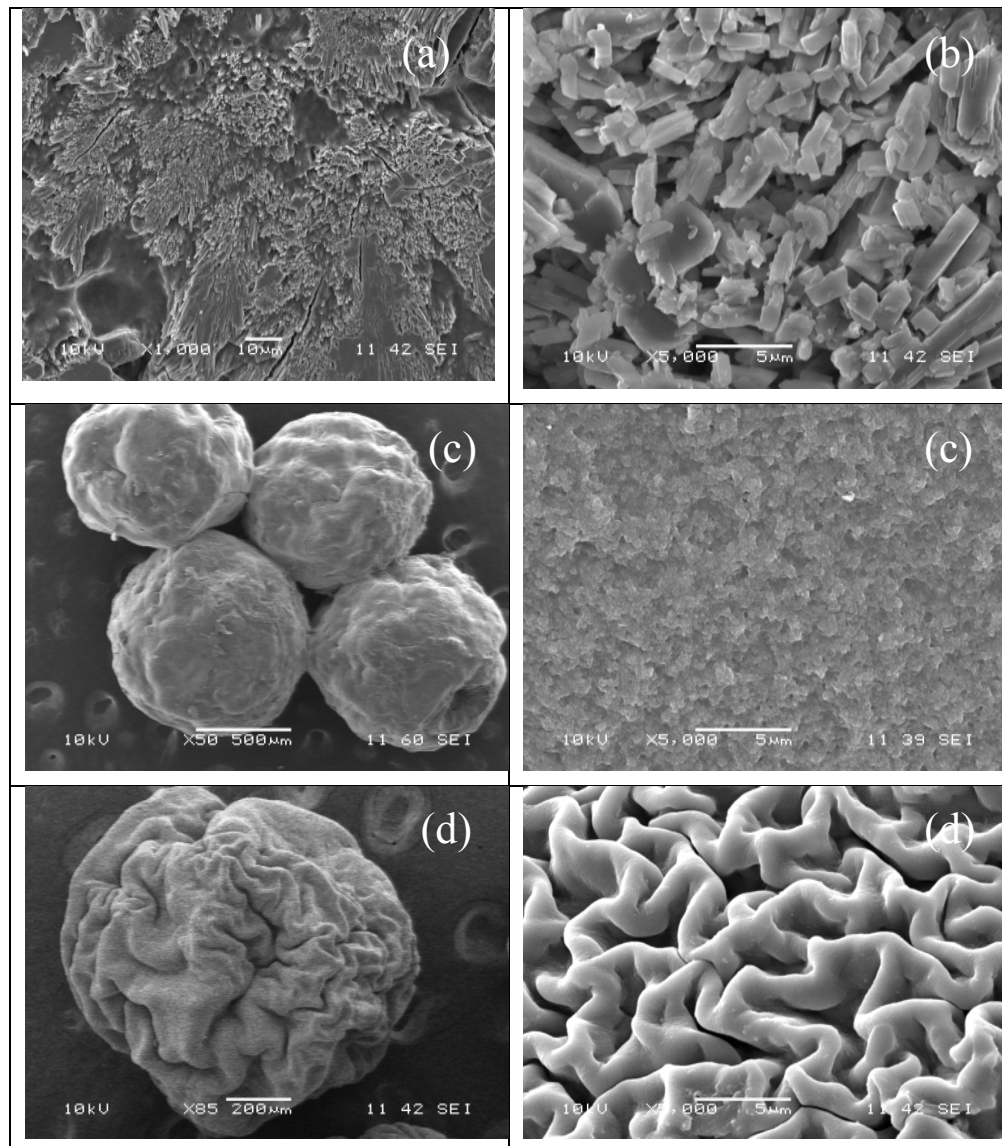


Fig. 1: SEM microphotographs of chitosan microcapsules cross-linked with TPP or HMP then with glutaraldehyde. (a) CS/TPP, (b) CS/HMP, (c) CS/TPP/GLU and (d) CS/HMP/GLU.

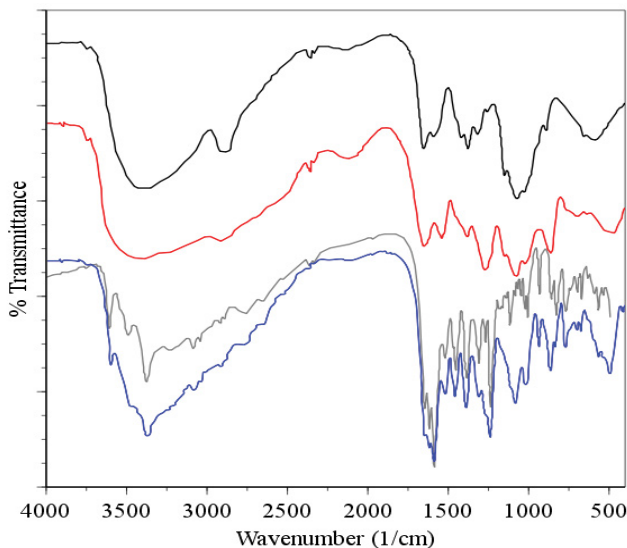


Fig. 2: FTIR spectra of chitosan microcapsules, chitosan microcapsules cross linked with hexametaphosphate (HMP), oxytetracycline and oxytetracycline-loaded chitosan microcapsules cross-linked with (HMP).

— Chitosan; — CS/HMP; — CS/OTC/HMP; — OTC.

of the primary amine group. The strong peak appearing at 1080 cm^{-1} is due to the skeletal vibrations involving the C-O stretching which are usually regarded as the fingerprint peak for the saccharide structure of CS while the peak at 1380 cm^{-1} corresponds to the alkane C-H stretching vibration^[30-33].

The spectra of cross-linked CS microspheres with HMP, (fig. 1b) and TPP (not represented) exhibit a strong and broadened antisymmetric band at about 3430 cm^{-1} , which results from overlapping of the O-H and N-H stretching vibrations of functional groups engaged in hydrogen bonds^[34]. Two absorption bands are observed in the spectrum of CS cross-linked with HMP: the band at 1654 cm^{-1} , (1654 cm^{-1} in TPP crosslinks) assigned to antisymmetric deformation of N-H vibrations in $-\text{NH}_3^+$ ion^[34,35] and the band at 1272 cm^{-1} (1215 cm^{-1} in TPP crosslinks) arising from P=O stretching vibrations in phosphate ions^[36], i.e. the antisymmetric stretching vibrations of PO_2^- groups. Such a vibration confirms the formation of ionic crosslinks between $-\text{NH}_3^+$ groups of CS and TPP ions^[35,37].

Comparison of the FTIR spectra of CS cross-linked with HMP or OTC (CS/HMP or CS/OTC in fig. 2) with the FTIR spectrum of the double cross-linked material CS/HMP/GLU (fig. 3) shows no significant difference except in the O-H and N-H stretching vibration regions ($1740\text{--}1720\text{ cm}^{-1}$). Indeed, the broad peak in this region is larger for CS/HMP/GLU than CS/HMP or CS/OTC likely due to more intense hydrogen bonds. Furthermore, the absence of characteristic

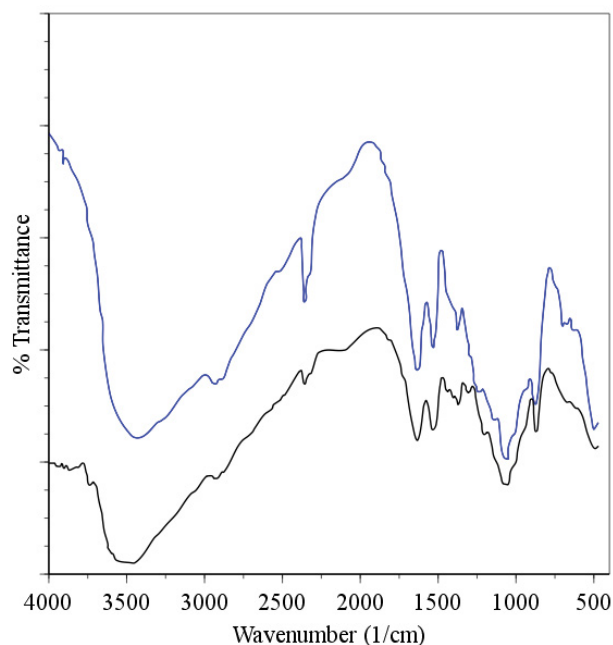


Fig. 3: FTIR spectra of double cross-linked chitosan microcapsules with TPP then GLU and with HMP then GLU.

— CS/TPP/GLU; — CS/HMP/GLU.

peaks of aldehyde in all spectra confirms that GLU has totally reacted with CS. The presence of the vibration bands located at 1272 , 1215 and 1257 cm^{-1} , in CS/HMP, CS/TPP/GLU and CS/HMP/GLU, respectively, is attributed to PO_2^- stretching vibrations whereas the peaks at 1651 cm^{-1} and 1647 cm^{-1} in CS/HMP/GLU and CS/TPP/GLU are assigned to the $-\text{NH}_2$ bending vibration indicating that HMP and TPP anions interact with $-\text{NH}_3^+$ cations of CS, respectively^[35,38].

The spectra of OTC and OTC-loaded CS microspheres cross-linked with HMP are presented in figs. 1c and 1d, respectively. The spectrum of OTC exhibits characteristic absorption bands at $1651\text{--}1589\text{ cm}^{-1}$ which arise from C=O and C=C bands of the aromatic cycle. The absorption band at 1650 cm^{-1} is attributed to $>\text{C}=\text{N}-\text{H}$ groups while the N-H and N-C vibrations bands of amine are located at 3487 cm^{-1} and 3371 cm^{-1} , respectively. The sharp band observed at around 3600 cm^{-1} comes from the stretching vibration of the free OH group and may be embedded with the absorption band of hydrogen-bonded hydroxyl groups which is usually broad in the $3550\text{--}3200\text{ cm}^{-1}$ region. The spectral analysis of OTC-loaded CS microspheres reveals the absorption bands between $1600\text{--}1500\text{ cm}^{-1}$ attributed to the OTC. In particular, vibration bands at 1630 , 1585 and 1334 cm^{-1} are assigned to amides, rotation vibration of aromatic C=CC and aromatic amines vibration, respectively. Furthermore, vibration bands located around 3602 , 3485 and 3371 cm^{-1} are observed

in the spectrum of OTC and CS/OTC/HMP as well. Therefore, FTIR spectra evidence that OTC does not react or interact significantly with CS or HMP after encapsulation in CS. The same conclusion is deduced with double cross-linked CS such as CS/OTC/HMP, CS/OTC/HMP/GLU and CS/GLU/OTC/HMP as depicted in fig. 4. The antibiotic agent OTC is therefore freely dispersed in the polymeric matrices.

Thermal analysis, DSC and TG analyses were carried out on the following microcapsules: (a) double cross-linked CS microcapsules with HMP followed by GLU on which diffusion of OTC was performed [(CS/HMP)+GLU×OTC], (b) cross-linked CS with HMP on which diffusion of OTC was performed [(CS/HMP)×OTC], (c) microcapsules obtained using CS mixed with OTC in the TPP coacervate before GLU cross-linking [(CS/OTC/TPP)/GLU] and (d) CS mixed with OTC in the coacervate TPP and GLU [(CS/OTC)(TPP/GLU)].

The DSC thermograms (not reported here) for the samples a, b and c showed an endothermic peak attributed to the evaporation of water in strong interaction with the hydrophilic cross-linked CS matrix. This evaporation leads to a weight loss percentage of 10% (ATG measurements) for samples a, b and c between 25 and 165° and nearly 15% for sample d between 25 and 195°. Material degradation occurs at higher temperature since the materials lose nearly 41% in weight when the temperature rises up to 400° for sample d and around 54% in weight for samples c, b and a. The thermal phenomena occurring during the material degradation are complex as depicted in fig. 5 where DTG curves of various samples are displayed.

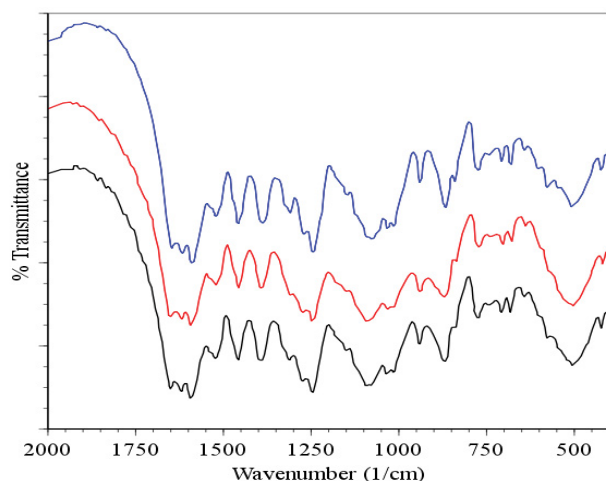


Fig. 4: FTIR spectra of oxytetracycline-loaded cross-linked CS microcapsules.
— CS/OTC/HMP; — (CS/OTC/HMP)/GLU; — (CS/GLU/OTC)/HMP.

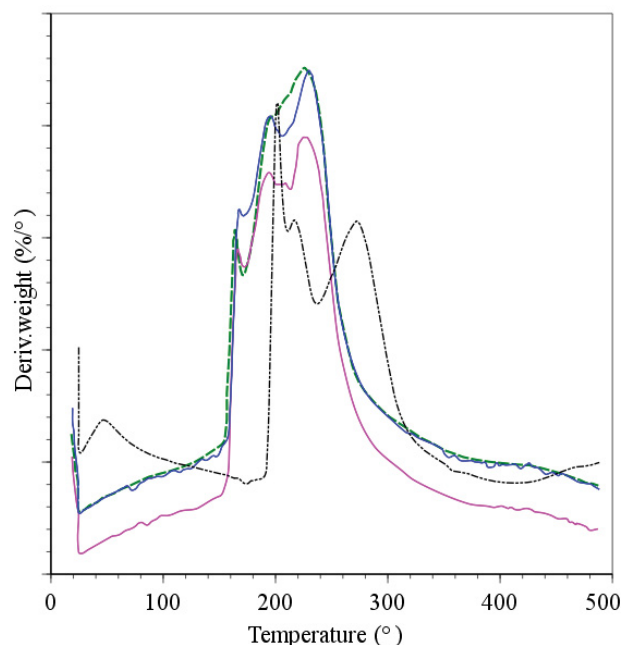


Fig. 5: TDG thermograms of various OTC containing cross-linked chitosan microcapsules.
— ((CS/OTC)(TPP/GLU)); — ((CS/OTC/TPP)/GLU); — ((CS/HMP)→OTC); — ((CS/HMP)/GLU→OTCCS).

They are likely due to simultaneous degradation of cross-linked CS and OTC. The exothermic thermal degradation of samples a-d occurs at lower temperature than the thermal degradation of CS that occurs between 250 and 350°^[39,40]. Therefore, it can be stated that the decrease of the thermal stability of cross-linked CS is due to the reduction of crystallinity. These results are in agreement with that reported by Kittur *et al.*^[41], which confirms by XRD, DSC, ICP and EDAX that a reduction in crystallinity and an increase in hydrophilicity of CS occur after cross-linking with TPP. The present work shows that the thermal stability decreases as: CS>CS/(TPP+GLU)>CS/TPP/GLU=CS/HMP=CS/HMP/GLU as reported in Pieróg *et al.*^[42] In conclusion, cross-linked CS membranes with GLU and TPP are less stable than CS. Besides, repeated TG measurements performed on sample d, for example, confirmed the good homogeneity of this sample.

Literature data shows that the thermal degradation of CS structure does not follow a single mechanism but is a complex reaction that gives different decomposition products^[43-46]. The decomposition starts from a random scission pathway of C-O-C bond of the pyranose ring and is followed by a further formation of small molecules and volatile compounds including acetic acid, acetic anhydride, acetamide and aromatic heterocycles such as pyrazines, pyridines, pyrroles and furans. However, it can be supposed that CS, cross-

linking agent and OTC in cross-linked microcapsules, release small molecular products under more complex thermal degradation behaviour. Thermal analysis of tetracycline hydrochloride^[47] showed an endothermic event at 225° and exothermic event at 235°, attributed to a fusion followed by thermal decomposition and oxidation of the evolved products.

In the present work, OTC release was investigated vs. time in buffered solutions simulating gastric media at pH 1.2 and pH 7.4. Preliminary tests for drug loading efficiency determination indicated that an average of 162.5 mg/g (drug/CS), i.e. 65% can be obtained for an initial charge of 250 mg/g. Examination of fig. 6 reveals that the OTC release kinetics exhibits an initial rapid release phase (s release) during a period of 5 h corresponding to the release of OTC entrapped at the surface of the CS microspheres. It appears that the drug release is faster at pH 1.2 (figs. 6a and 6b) than at pH 7.4 (figs. 6c and 6d) and in the presence of HMP as cross-linking agent. In fact, 49.5% OTC was released with (CS/OTC)/HMP compared to 45.5% OTC with (CS/

OTC)/TPP at pH 1.2 while 40.2% OTC was released with (CS/OTC)/HMPS compared to 30.2% OTC with (CS/OTC)/TPP at pH 7.4. Expanded release stage is obtained with the double cross-linked CS beads (CS/OTC/TPP)/GLU (27.1% at pH 1.2 and 12.6% at pH 7.4). The curves presented in fig. 6 show that the burst period is followed by sustainable and slow release phase giving highest cumulative drug amount. For example, 81.7% and 50.3% OTC was released after 25 h at pH 1.2 and pH 7.4 with (CS/OTC)/TPP, respectively, while 82.7% and 66.1% OTC was released at pH 1.2 and pH 7.4 with (CS/OTC)/HMP, respectively. The influence of pH on the OTC release can be attributed to the highest OTC solubility in acidic media and more important polymeric matrix erosion in such media.

Comparison of the matrix type release system, where OTC molecules are uniformly dispersed within the polymer matrices, shows that CS/HMP systems improve OTC release kinetics in relation to the CS/TPP systems. Addition of GLU as a second cross-linking agent increases the rigidity and the density of the CS

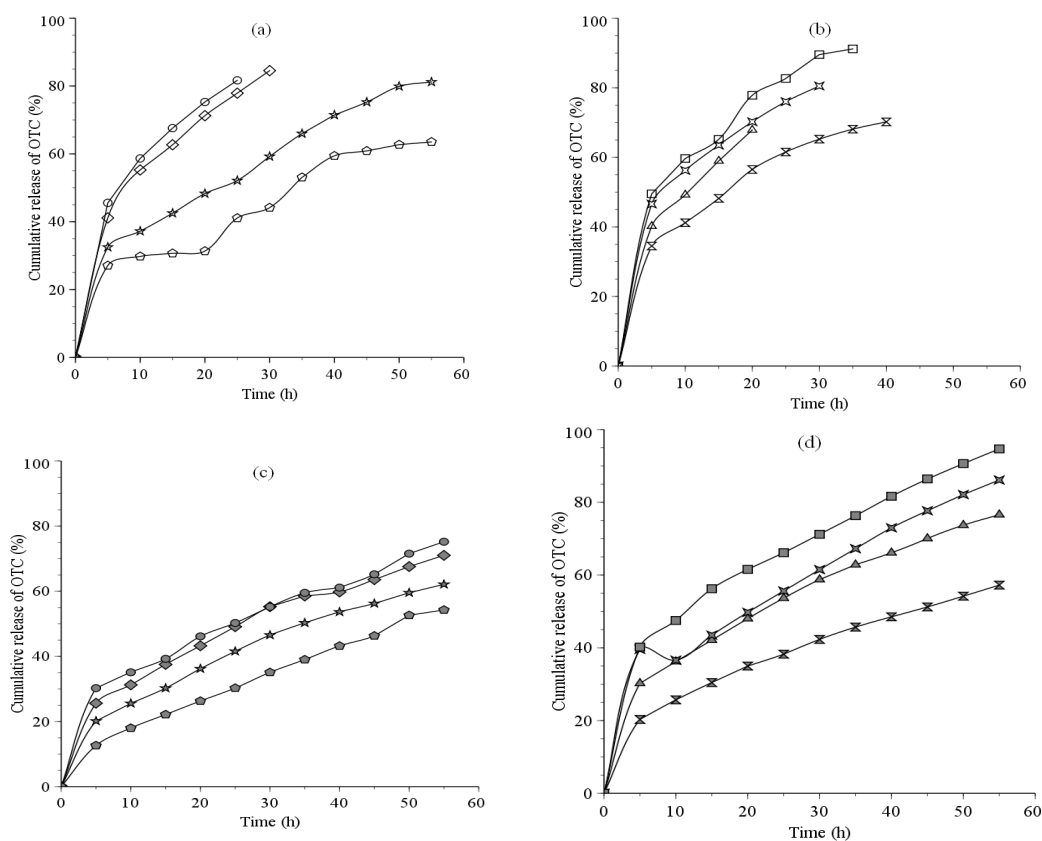


Fig. 6: Isothermal (37°) *in vitro* release kinetic profiles of OTC from CS microcapsules in simulated biological fluids at pH 7.4 and pH 1.2.

(a) and (b) Release profiles from loaded CS/TPP and CS/HMP cross-linked microcapsules at pH 1.2; (c) and (d) release profiles from loaded CS/TPP and CS/HMPS cross-linked microcapsules at pH=7.4.

-□- (CS/OTC)/HMP, -x- (Cs/OTC/GLU)/HMP, -▲- (CS/OTC)/(HMP)/GLU, -◆- (CS/OTC)/HMP)/GLU -●- (CS/OTC)/TPP, -♦- (Cs/OTC/GLU)/TPP, -⊙- (CS/OTC)/(TPP)/GLU, -△- (CS/OTC/TPP)/GLU.

membrane and, thus, reduces OTC diffusion from the polymeric network, particularly when GLU is used during the final treatment, i.e. in (CS/OTC/HMP)/GLU or in (CS/OTC/TPP)/GLU. The release percentage was lowered down to 52% for (CS/OTC/HMP)/GLU and nearly 18% for (CS/OTC/TPP)/GLU.

Swelling measurements (not shown here) on the various OTC carrying systems were found to be consistent with the release kinetics yields discussed above. In general, the polymer reticulation greatly lowers the degree of swelling^[48]. The swelling behaviour, which can be attributed to the presence of ionisable groups within the gel structure^[48,49], was obviously pH dependent and varying with CS cross-linking features. The lowest swelling level was found with double cross-linked CS beads as in (CS/OTC/TPP)/GLU, (CS/OTC/GLU)/HMP and (CS/OTC)/(HMP/GLU) formulations and GLU free matrices such as (CS/OTC)/TPP or (CS/OTC)/HMP give rise to highest swelling content. The TPP systems are found to swell better at pH 7.4, whereas, HMP systems swell better at pH 1.2. For both pH, the swelling capacity decreases in the order, (CS/OTC)/X>(CS/OTC/GLU)/X>(CS/OTC)/(X/GLU)>(CS/OTC/X)/GLU, where X=TPP or HMP.

The release kinetic curves given in fig. 6 are consistent with a multi-step model in which diffusion of the drug from the membrane and the bulk degradation of the polymer may be the control parameters^[50]. However, to investigate the mechanism of drug release from the microcapsules and due the fact that in most cases the theoretical concepts does not exist, the release data were

analyzed using various empirical or semi-empirical equations which have proved to be very appropriate. Most of the mathematical models commonly used to determine the drug release from carrying dosage forms are listed in recent literature^[29,51,52].

Preliminary calculations (data not shown) indicate that zero order, first order and Hopfenberg model kinetics were not satisfactory by fitting the experimental release data that have been obtained. The correlation coefficient value R^2 found with these models was under 0.95. Diffusion controlled release following Higuchian kinetics or the derived equation of Baker-Lonsdale are consistent with the experimental results which indicate that the dissolution of drug occurs after effectively enclosed polymeric matrix and is not ready to dissolve from carrier surface. However, correlation coefficient less than 0.99 indicates that the drug release behaviour is not governed by the diffusion mechanism only^[53]. Satisfactory correlation is also given with the Weibull equation which is however an empiric model. By far, the Makoid-Banakar, Peppas-Sahlin and Korsmeyer-Peppas equations provide the best fit as depicted in Table 2 and since these models fit very well the release data, it is possible to elucidate the mechanism of OTC release from the obtained carrying beads. Combination of more than one type of release phenomenon could be involved here. At first consideration, the release process can be driven by Fick diffusion and polymeric matrix relaxation and erosion in agreement with Korsmeyer-Peppas model, for example, when the polymer matrix swells the mobility of the chains increases allowing an easy penetration of the solvent. Thus, the Kick

TABLE 2: RELEASE RATE CONSTANTS WITH CORRELATION COEFFICIENT (R^2) FOR MODEL EQUATIONS FITTING OF OTC RELEASE DATA

| model | pH 1.2 | | | | pH 7.4 | | | | |
|-------------------------------------|-----------------------------|-------------------------|--------------------------|--------------------------|------------------------------|-------------------------|-------------------------|--------------------------|--|
| | (Cs/OTC)/ TPP | (Cs/OTC/ TPP)/Glu | (Cs/OTC)/(TPP/ Glu) | (Cs/OTC/GLU)/ TPP | (Cs/OTC)/ TPP | (Cs/OTC/TPP)/ Glu | (Cs/OTC)/(TPP/ Glu) | (Cs/OTC/GLU)/ TPP | |
| Higuchi K_H | (0.9795) 17.25 | (0.9560) 8.71 | (0.9862) 11.12 | (0.9868) 16.01 | (0.9825) 10.09 | (0.9646) 6.73 | (0.9971) 8.37 | (0.9939) 9.69 | |
| Weibull 1 $\alpha; B$ | (0.9984) 4.67; 0.63 | (0.9438) 14.98; 0.67 | (0.9719) 11.44; 0.71 | (0.9961) 5.93; 0.68 | (0.9802) 9.65; 0.61 | (0.9909) 44.75; 0.88 | (0.9947) 16.49; 0.69 | (0.9928) 11.71; 0.65 | |
| Peppas- Sahlin1 $K_1; K_2 m$ | (1.0000) 25.14; 0.65 | (0.9595) 8.27; 1.48 | (0.9901) 11.74; 2.20 | (0.9995) 20.07; 2.82 | (0.9925) 11.87; 2.31 | (0.9973) 4.01; 0.45 | (0.9977) 6.83; 2.26 | (0.9970) 9.89; 2.65 | |
| Peppas- Sahlin2 $K_1; K_2$ | (0.9994) 22.87; -1.34 | (0.9566) 8.303; 0.07 | (0.9869) 11.66; -0.09 | (0.9988) 19.84; -0.84 | (0.9879) 11.480; -0.23 | (0.9973) 4.01/0.45 | (0.9975) 8.05; 0.05 | (0.9963) 10.61; -0.15 | |
| Korsmeyer- Peppas $K_{kp}; n$ | (1.0000) 25.41; 0.36 | (0.9561) 8.64; 0.50 | (0.9879) 12.54; 0.47 | (0.9995) 21.71; 0.40 | (0.9907) 12.98; 0.43 | (0.9955) 3.53; 0.68 | (0.9974) 7.95; 0.51 | (0.9966) 11.25; 0.46 | |
| Baker- Lonsdale K_{BL} | (0.9989) 0.008 | (0.9455) 0.002 | (0.9768) 0.003 | (0.9984) 0.007 | (0.9864) 0.002 | (0.9434) 0.001 | (0.9882) 0.002 | (0.9937) 0.002 | |
| Makoid- Banakar $K_{MB}; n$ | (1.0000) 25.68; 0.35 | (0.9690) 16.64; 0.19 | (0.9945) 19.17; 0.26 | (0.9996) 22.79; 0.37 | (0.9975) 19.27; 0.24 | (0.9984) 5.44; 0.49 | (0.9975) 8.41; 0.50 | (0.9968) 12.06; 0.42 | |

diffusion of the entrapped substrate is dependent on the solvent diffusion velocity, which is considered to be smaller than the polymeric relaxation velocity^[54,55].

CS microcapsules used as carriers and delivery systems for OTC have been characterized and the effect of different formulations on the drug release behaviour has been investigated. FTIR spectroscopy indicates the formation of ionic crosslinks between CS and anionic groups of TPP and HMP and characteristic FTIR bands of OTC observed in loaded blends suggest that the antibiotic is dispersed freely within the microcapsule without any significant interactions. This result has been confirmed by DSC experiments which evidenced the occurrence of homogeneous preparations. The successful release extent of OTC from cross-linked CS beads is affected significantly by pH and cross-linking agent. Makoid-Banakar, Peppas-Sahlin and Korsmeyer-Peppas models lead to the best fit of experimental data, indicating that the release process may be governed by concomitance of various phenomena like drug dissolution and diffusion, swelling, relaxation and erosion of the polymeric matrix.

Conflict of interest:

There is no potential conflict of interest.

Financial support and sponsorship:

Nil.

REFERENCES

- Chopra I, Roberts M. Tetracycline antibiotics: mode of action, applications, molecular biology, and epidemiology of bacterial resistance. *Microbiol Mol Biol Rev* 2001;65:232-60.
- Dax SL. Antibacterial chemotherapeutic agents. London: Blackie Academic and Professional; 1997.
- Finch RG. Tetracyclines, In: Grady FO', Lambert HP, Finch RG, Greenwood D, editors. *Antibiotic and Chemotherapy*, 7th ed. Philadelphia: WB Saunders Company; 1997.469-84.
- Schnappinger D, Hillen W. Tetracyclines: antibiotic action, uptake, and resistance mechanisms. *Arch Microbiol* 1996;165:359-69.
- Sendil D, Gursel I, Wise DL, Hasýrcý V. Antibiotic release from biodegradable PHBV microparticles. *J Control Release* 1999;59:207-17.
- Hejazi R, Amiji M. Stomach specific anti *H. pylori* therapy. I: preparation and characterization of tetracycline loaded chitosan microspheres. *Int J Pharm* 2002;235:87-94.
- Cruz MC, Ravagnani SP, Brogna FM, Campana SP, Triviño GC, Lisboa AC. Evaluation of the diffusion coefficient for controlled release of oxytetracycline from alginate/chitosan/poly (ethylene glycol) micro beads in simulated gastrointestinal environments. *Biotechnol Appl Biochem* 2004;40:243-53.
- Ta HT, Dass CR, Dunstan DE. Injectable chitosan hydrogels for localised cancer therapy. *J Control Release* 2008;126:205-16.
- Ravi Kumar MNV, Bakowsky U, Lehr CM. Preparation and characterization of cationic PLGA nanospheres as DNA carriers. *Biomaterials* 2004;25:1771-7.
- Felt O, Gurny R, Baeyens V. Delivery of antibiotics to the eye using a positively charged polysaccharide as vehicle. *AAPS PharmSci* 2001;3:87-93.
- Maestrelli F, Garcia-Fuentes M, Mura P, Jose' Alonso M. A new drug nanocarrier consisting of chitosan and hydroxypropylcyclodextrin. *Eur J Pharm Biopharm* 2006;63:79-86.
- Giri TK, Thakur A, Alexander A, Badwaik H, Tripathi DK. Modified chitosan hydrogels as drug delivery and tissue engineering systems: present status and applications. *Acta Pharmaceutica Sinica B* 2012;2:439-49.
- Patel MP, Patel RR, Patel JK. Chitosan mediated targeted drug delivery system: A Review. *J Pharm Pharmaceut Sci* 2010;13:536-57.
- Riva R, Ragelle H, des Rieux A, Duhem N, Jérôme C, Préat V. Chitosan and chitosan derivatives in drug delivery and tissue engineering in. *Adv Polym Sci* 2011;244:19-44.
- Sonia TA, Sharma CP. Chitosan and its derivatives for drug delivery perspective. *Adv Polym Sci* 2011;243:23-54.
- Shashiwa H, Shegemasa Y, Roy R. Chemical modification of chitosan 11: chitosan-dendrimer hybrid as a tree like molecule. *Carbohydr Polym* 2002;49:195-205.
- Dastan T, Turan K. *In vitro* characterization and delivery of chitosan DNA microcapsules into mammalian cells. *J Pharm Pharm Sci* 2004;7:205-14.
- George M, Abraham TE. Polyionic hydrocolloids for the intestinal delivery of protein drugs: Alginate and chitosan: a review. *J Control Release* 2006;114:1-14.
- Hejazi R., Amiji M. Stomach specific anti *H. pylori* therapy part III: Effect of chitosan microspheres crosslinking on the gastric residence and local tetracycline concentrations in fasted gerbils. *Int J Pharm* 2004;272:99-108.
- Berger J, Reist M, Mayer JM, Felt O, Peppas NA, Gurny R. Structure and interactions in covalently and ionically crosslinked chitosan hydrogels for biomedical applications. *Eur J Pharm Biopharm* 2004;57:19-34.
- Ko JA, Park HJ, Hwang SJ, Park JB, Lee JS. Preparation and characterization of chitosan microparticles intended for controlled drug delivery. *Int J Pharma* 2002;249:165-74.
- Shu XZ, Zhu KJ. A novel approach to prepare tripolyphosphate/chitosan complex beads for controlled release drug delivery. *Int J Pharma* 2000;201:51-8.
- Gupta KC, Jabrail FH. Preparation and characterization of sodium hexametaphosphate cross linked chitosan microspheres for controlled and sustained delivery of centchroman. *Int J Biol Macromol* 2006;38:272-83.
- Kleine-Brueggeney H, Zorzi GK, Fecker T, El Gueddari NE, Moerschbacher BM, Goycoolea FM. A rational approach towards the design of chitosan based nanoparticles obtained by ionotropic gelation. *Colloids Surf Biointerfaces* 2015;135:99-108.
- Saccoa P, Paoletta S, Coka M, Asarob F, Abramic M, Grassid M, *et al.* Insight into the ionotropic gelation of chitosan using tripolyphosphate and pyrophosphate as cross-linkers. *Int J Biol Macromol* 2016;92:476-83.
- Patel MA, Abou Ghaly MHH, Schryer-Praga JV, Chadwick K. The effect of ionotropic gelation residence time on alginate cross-linking and properties. *Carbohydr Polym* 2017;155:362-71.
- Pati F, Adhikari B, Dhara S. Development of chitosan-tripolyphosphate fibers through pH dependent ionotropic gelation. *Carbohydr Res* 2011;346:2582-8.

28. Leong JY, Lam WH, Ho KW, Voo WP, Lee MFX, Lima HP, *et al.* Advances in fabricating spherical alginate hydrogels with controlled particle designs by ionotropic gelation as encapsulation systems. *Particuology* 2016;24:44-60.
29. Yong Z, Meirong H, Jianping Z, Aifeng Z, Weize L, Chengli Y. An add-in program for modeling and comparison of drug dissolution profiles. *AAPS J* 2010;12:263-71.
30. Peniche-Covas C, Argüelles-Monal W, Román JS. A kinetic study of the thermal degradation of chitosan and a mercaptan derivative of chitosan. *Polym Degrad Stab* 1993;39:21-28.
31. Britto D, Campana-Filho SG. A kinetic study on the thermal degradation of N,N,N-trimethylchitosan. *Polym Degrad Stab* 2004;84:353-61.
32. Neto CGT, Giacometti JA, Job AE, Ferreira FC, Fonseca JLC, Pereira MR. Thermal analysis of chitosan based networks. *Carbohydr Polym*, 2005;62:97-103.
33. Pawlak A, Mucha. Thermogravimetric and FTIR studies of chitosan blends. *Thermochim Acta* 2003;396:153-66.
34. K Nakamoto. Infrared and Raman Spectra of Inorganic and Coordination Compounds, Part A Theory and Applications in Inorganic Chemistry. 6th ed. Hoboken, NJ: Wiley Interscience; 2008.
35. Pieróg M, Gierszewska-Drużyńska M, Ostrowska-Czubenko J. Effect of ionic crosslinking agents on swelling behaviour of chitosan hydrogel membranes. *PCACD* 2009;14:75-82.
36. He Z, Honeycutt CW, Xing B, McDowel RW, Pellechia PJ, Zhang T. Solid-state Fourier transform infrared and ³¹P nuclear magnetic resonance spectral features of phosphate compounds. *Soil Sci* 2007;172:501-15.
37. Gierszewska-Drużyńska M, Ostrowska-Czubenko J. The effect of ionic crosslinking on thermal properties of hydrogel chitosan membranes. *PCACD* 2010;15:25-32.
38. Ribeiro AJ, Silva C, Ferreira D, Veiga F. Chitosan-reinforced alginate microspheres obtained through the emulsification/internal gelation technique. *Eur J Pharm Sci* 2005;25:31-40.
39. Sakurai K, Maegawa T, Takahashi T. Glass transition temperature of chitosan and miscibility of chitosan/poly (N-vinyl pyrrolidone) blends. *Polymer* 2000;41:7051-6.
40. Zeng M, Fang Z, Xu C. Effect of compatibility on the structure of the microporous membrane prepared by selective dissolution of chitosan/synthetic polymer blend membrane. *J Membr Sci* 2004;230:175-81.
41. Kittur FS, Harish Prashanth KV, Udaya Sankar K, Tharanathan RN. Characterization of chitin, chitosan and their carboxymethyl derivatives by differential scanning calorimetry. *Carbohydr Polym* 2002;49:185-93.
42. Pieróg M, Ostrowska-Czubenko J, Gierszewska-Drużyńska M. Thermal degradation of double cross-linked hydrogel chitosan membranes. *PCACD* 2012;17:67-74.
43. Wanjun T, Cunxin W, Donghua Ch. Kinetic studies on the pyrolysis of chitin and chitosan. *Polym Degr Stab* 2005;87:389-94.
44. Lopez FA, Merce ALR, Alguacil FJ, Lopez-Delgado A. A kinetic study on the thermal behaviour of chitosan. *J Therm Anal Calorim* 2008;91:633-9.
45. Zawadzki J, Kaczmarek H. Thermal treatment of chitosan in various conditions. *Carbohydr Polym* 2011;89:395-401.
46. Zeng L, Qin C, Wang L, Li W. Volatile compounds formed from the pyrolysis of chitosan. *Carbohydr Polym* 2011;83:1553-7.
47. Fernandes NS, Filho MASC, Mendes RA, Ionashiro M. Thermal Decomposition of Some Chemotherapeutic Substances. *J Braz Chem Soc* 1999;10:459-62.
48. Mao J, Kondu S, Ji H-F, McShane MJ. Study of the near-neutral pH-sensitivity of chitosan/gelatin hydrogels by turbidimetry and microcantilever deflection. *Biotechnol Bioeng* 2006;95:333-41.
49. Ray M, Pal K, Anis A, Banthia AK. Development and Characterization of Chitosan-Based Polymeric Hydrogel Membranes. *Des Monomers Polym* 2010;13:193-206.
50. Siegel RA, Rathbone MJ. Overview of controlled release mechanisms. In: Siepmann J, Siegel RA, Rathbone MJ, editors. *Fundamentals and Applications of Controlled Release Drug Delivery*. New York: Springer US; 2012. p.19-43.
51. Pepas NA, Sahlin JJ. A simple equation for the description of solute release III: Coupling of diffusion and relaxation. *Int J Pharm*, 1989;57:169-72.
52. Makoid MC, Dufour A, Banakar UV. Modelling of dissolution behaviour of controlled release systems. *STP Pharma* 1993;3:49-58.
53. Pardakhty A, Varshosaz J, Rouholamini A. *In vitro* study of polyoxyethylene alkyl ether niosomes for delivery of insulin. *Int J Pharm* 2007;328:130-41.
54. Masaro L, Zhu XX. Physical models of diffusion for polymer solutions, gels and solids. *Prog Polym Sci* 2007;24:731-75.
55. Ritger PL, Peppas NA. A simple equation for description of solute release. Fickian and anomalous release from swellable devices. *J Control Release* 1987;5:37-42.